ARCHIVES OF ACOUSTICS
34, 1, 51–61 (2009)

Triangular Bézier Patches in Modelling Smooth Boundary Surface in exterior Helmholtz Problems Solved by the PIES

Eugeniusz ZIENIUK, Krzysztof SZERSZEŃ

University of Białystok
Faculty of Mathematics and Computer Science
Sosnowa 64, 15-887 Białystok, Poland
e-mail: ezieniuk@ii.uwb.edu.pl, kszerszen@ii.uwb.edu.pl

(*received March 15, 2008; accepted January 22, 2009*)

The paper proposes the use of triangular parametric Bézier patches as a new and effective way to generate three-dimensional boundaries in acoustics problems. The boundary geometry composed of triangular Bézier patches has been directly linked to the parametric integral equation system (PIES) to numerical solving exterior Helmholtz problems. A primary advantage of the proposed approach is to avoid the necessity of conventional domain or boundary discretization. The obtained numerical solutions compared with literature exacts results are characterized by high accuracy and convergence.

Keywords: Helmholtz equation, acoustics problems, the parametric integral equation system (PIES), triangular Bézier patches.

1. Introduction

Solving acoustics problems often involves conducting a detailed analysis of solutions in infinite (exterior) domains. Taking into consideration infinite domains in the finite element method (FEM) is highly problematic. In practice, this leads to discretization into finite-elements large but still finite domains [10]. The boundary element method (BEM), another widespread numerical method, appears to be a more suitable approach for solving exterior problems than the FEM. The BEM [1, 4, 5] is based on the boundary integral equation (BIE) in which only the boundary of the domain is needed to be discretized into elements. In order to apply the BEM to exterior problems, only the interior boundary is discretized. The BEM, in spite of decreased number of used elements in comparison with the FEM, has also its disadvantages mainly because of the lack in satisfying automatic continuity at joining nodes of boundary elements.

It must be noted that any shape modification of the boundary, results in a rediscretication of the existing element structure of the geometry. Additionally, the BEM solutions are obtained at the declared nodes. Therefore, in order to improve the accuracy and verify the convergence of solutions should be increased the number of boundary elements, which leads to the declaration of additional nodes.

In our own research a new approach for numerical solving of two and three dimensional boundary problems was proposed. As a result of the analytical modification of the classical BIE a new parametrical integral equation system (PIES) was obtained. The proposed approach has been successfully applied to a variety of two-dimensional problems with different character (Laplace [6], Hemlholtz [7], Navier–Lamé [8] equations). In the case of 3D problems only preliminary analysis of the PIES application for Helmholtz problems has been conducted for the domains with polygonal boundaries defined by flat rectangular Coons surfaces [9]. The primary objective of this paper is to apply triangular Bézier patches for modelling boundary geometry in the PIES in the case of 3D Helmholtz problems. The obtained numerical solutions were compared with literature exact results.

2. Triangular Bézier patches in creating three-dimensional representation of the boundary

The rapid development of computer graphics has brought progress in a visual representation of complex 2D and 3D geometries. One of the main tools widely used in computer graphics applications appear to be parametric curves and surfaces. The parametric representation is well-known in the computer graphics community, and has matured into a powerful tool designed for modelling and visualization.

Triangular Bézier surfaces of order n is declared by a set of $0.5(n+1)(n+2)$ control points P_{ijk} for integer indices i, j, k and $i+j+k=n$. Figure 1 shows sample patches of 3rd and 4th degree defined by 10 and 15 control points, respectively.

The formula for the surface defined by these control points is written as a mapping of the triangle in the 2-D parameter space $0 \leq v, w, u \leq 1$ and $v+w+u \leq 1$ into the 3D space of the control points as presented below [2, 3]

$$P^n(v,w,u) = \sum_{i,j,k \geq 0} P_{i,j,k} B^n_{i,j,k}(v,w,u), \tag{1}$$

where

$$B^n_{i,j,k}(v,w,u) = \begin{pmatrix} n \\ i,j,k \end{pmatrix} v^i w^j u^k = \frac{n!}{i!\,j!\,k!} v^i w^j u^k, \tag{2}$$

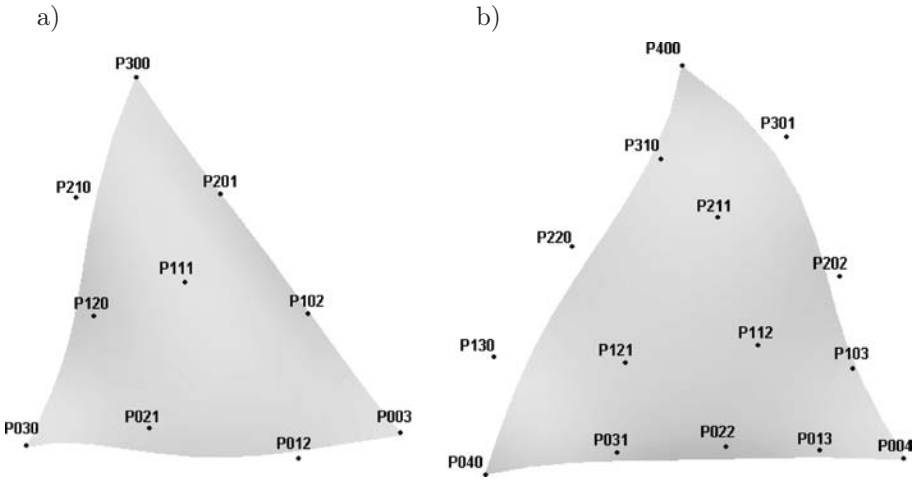

Fig. 1. Triangular Bézier patches of 3rd (a) and 4th (b) degree with control points.

is a Bernstein polynomial. The complete expressions for the triangular Bézier patches of 3rd and 4th degree shown in Fig. 1 are written as

$$\begin{aligned} P^3(u,v,w) = {} & w^3P_{003} + 3vw^2P_{012} + 3v^2wP_{021} + v^3P_{030} \\ & + 3uw^2P_{102} + 6uvwP_{111} + 3uv^2P_{120} \\ & + 3u^2wP_{201} + 3u^2vP_{210} \\ & + u^3P_{300}, \end{aligned} \tag{3}$$

and

$$\begin{aligned} P^4(u,v,w) = {} & w^4P_{004} + 4vw^3P_{013} + 6v^2w^2P_{022} + 4v^3wP_{031} + v^4P_{040} \\ & + 4uw^3P_{103} + 12uvw^2P_{112} + 12uv^2wP_{121} + 4uv^3P_{130} \\ & + 6u^2w^2P_{202} + 12u^2vwP_{211} + 6u^2v^2P_{220} \\ & + 4u^3wP_{301} + 4u^3vP_{310} \\ & + u^4P_{400}. \end{aligned} \tag{4}$$

After substitution $u = 1 - v - w$ in (1) and additional restrictions imposed on $0 \leq v, w \leq 1$ and $v + w \leq 1$ the surface of Bézier patch can be mapped by two only parameters v, w. In this case, expressions (1), (2) may be reduced to

$$P^n(v,w) = \sum_{i,j,k \geq 0} P_{i,j,k} B^n_{i,j,k}(v,w,1-v-w) \tag{5}$$

and

$$\begin{aligned} & B^n_{i,j,k}(v,w,1-v-w) = \\ & \qquad \binom{n}{i,j,k} v^i w^j (1-v-w)^k = \frac{n!}{i!\,j!\,k!} v^i w^j (1-v-w)^k . \end{aligned} \tag{6}$$

The above formulas for Bézier patches will be used in the rest of the paper.

3. The PIES for Helmholtz equation in domain bounded by triangular Bézier surfaces

The boundary in this paper is shaped by means of discussed in previous section triangular Bézier patches. We can easy join individual patches together to form smooth closed surface. The boundary, being thus described, is explicitly taken into consideration in presented below mathematical formula of the PIES [9]

$$0.5u_l(v_1,w_1) = \sum_{j=1}^{n} \int_{v_{j-1}}^{v_j} \int_{w_{j-1}}^{w_j} \left\{ \overline{U}^*_{lj}(v_1,w_1,v,w)p_j(v,w) - \overline{P}^*_{lj}(v_1,w_1,v,w)u_j(v,w) \right\} J_j(v,w)\,\mathrm{d}v\,\mathrm{d}w \tag{7}$$

and $v_{j-1} < v_1,\ v < v_j;\ w_{j-1} < w_1,\ w < w_j;\ l = 1,2,3...n$, exactly in functions $\overline{U}^*_{lj}$ and $\overline{P}^*_{lj}$

$$\overline{U}^*_{lj} = \begin{bmatrix} \mathrm{Re}\{U^*_{lj}\} & -\mathrm{Im}\{U^*_{lj}\} \\ \mathrm{Im}\{U^*_{lj}\} & \mathrm{Re}\{U^*_{lj}\} \end{bmatrix}, \tag{8}$$

where

$$U^*_{lj} = \frac{1}{4\pi\eta} e^{ik\eta} = \frac{1}{4\pi\eta}\left\{\cos k\eta + i \sin k\eta\right\}$$

and

$$\overline{P}^*_{lj} = \begin{bmatrix} \mathrm{Re}\{P^*_{lj}\} & -\mathrm{Im}\{P^*_{lj}\} \\ \mathrm{Im}\{P^*_{lj}\} & \mathrm{Re}\{P^*_{lj}\} \end{bmatrix}, \tag{9}$$

where

$$P^*_{lj} = \frac{\partial U^*_{lj}}{\partial n} = \frac{1}{4\pi\eta^3}\left\{(\cos k\eta + k\eta \sin k\eta) + i\,(\sin k\eta - k\eta\cos k\eta)\right\}\left\{\eta_1 n_1 + \eta_2 n_2 + \eta_3 n_3\right\}.$$

This formula of the PIES is similar to the previously presented one, where the PIES approach was studied for interior polygonal domains bounded by rectangular Coons patches [9]. The difference lies in the adaptation of the PIES formula for considerably more complicated than previously used flat Coons surfaces – new smooth Bézier patches in

$$\begin{aligned} \eta_1 &= P_{l\{x_1\}}(v_1,w_1) - P_{j\{x_1\}}(v,w), \\ \eta_2 &= P_{l\{x_2\}}(v_1,w_1) - P_{j\{x_2\}}(v,w), \\ \eta_3 &= P_{l\{x_3\}}(v_1,w_1) - P_{j\{x_3\}}(v,w), \\ \eta(v,w) &= [\eta_1^2 + \eta_2^2 + \eta_3^2]^{0.5}. \end{aligned} \tag{10}$$

It is possible to insert into (10) Bézier patches of any degree expressed by (5). In the paper the patches of 4th degree will be used. The smooth character of Bézier surfaces requires new attitudes about computing the Jacobian $J_j(v,w)$ in (7) and normal derivatives $n_1(v,w)$, $n_2(v,w)$, $n_3(v,w)$ in (9). In the case of previously used flat Coons patches the Jacobian and normal derivatives were constant on the whole surface area regardless of the actual values for parameters v, w. Currently, these parameters change at any point of the patch, depending on changes of v, w. A new formula for the Jacobian and normal derivatives can be determined analytically from expressions (5) and (6) that define triangular surfaces as follows

$$n_m(v,w) = \frac{A_m(v,w)}{J_j(v,w)}, \qquad m = 1,2,3, \tag{11}$$

where

$$\begin{aligned}
A_1(v,w) &= \frac{\partial P_{j\{x2\}}(v,w)\partial P_{j\{x3\}}(v,w)}{\partial w \partial v} - \frac{\partial P_{j\{x2\}}(v,w)\partial P_{j\{x3\}}(v,w)}{\partial v \partial w}, \\
A_2(v,w) &= \frac{\partial P_{j\{x3\}}(v,w)\partial P_{j\{x1\}}(v,w)}{\partial w \partial v} - \frac{\partial P_{j\{x3\}}(v,w)\partial P_{j\{x1\}}(v,w)}{\partial v \partial w}, \\
A_3(v,w) &= \frac{\partial P_{j\{x1\}}(v,w)\partial P_{j\{x2\}}(v,w)}{\partial w \partial v} - \frac{\partial P_{j\{x1\}}(v,w)\partial P_{j\{x2\}}(v,w)}{\partial v \partial w},
\end{aligned} \tag{12}$$

and

$$J_j(v,w) = [A_1^2(v,w) + A_2^2(v,w) + A_3^2(v,w)]^{0.5}. \tag{13}$$

The appropriate (outward or inward) direction of normal derivatives $n_1(v,w)$, $n_2(v,w)$, $n_3(v,w)$ is determined by the appropriate clockwise or anticlockwise numeration of control points of Bézier patches. In the case of solving exterior boundary value problems and to obtain outward direction of normal derivatives, each controls points will be numbered in clock directions.

The numerical method for solving the PIES with the boundary represented by triangular patches is identical to the previously used in the case of rectangular Coons surfaces [9]. Boundary functions $u_j(v,w)$, $p_j(v,w)$ from integral Eq. (7) are defined on each Bézier patch j by means of the following series

$$u_j(v,w) = \sum_{p=0}^{N}\sum_{r=0}^{M}\left\{r_j^{(pr)} + is_j^{(pr)}\right\} T_j^{(p)}(v) T_j^{(r)}(w), \tag{14}$$

$$p_j(v,w) = \sum_{p=0}^{N}\sum_{r=0}^{M}\left\{u_j^{(pr)} + iv_j^{(pr)}\right\} T_j^{(p)}(v) T_j^{(r)}(w), \tag{15}$$

where $\overline{n} = N \times M$ – the number of coefficients on each Bézier surface, $T_j^{(p)}(v)$, $T_j^{(r)}(w)$ – the global base functions – Chebyshev polynomials, $u_j^{(pr)}$, $v_j^{(pr)}$, $r_j^{(pr)}$, $s_j^{(pr)}$ – the unknown coefficients, whose values are obtained by pseudospectral collocation method [9].

4. Solution in the exterior domain

After obtaining a complete representation of boundary functions $u_j(v,w)$, $p_j(v,w)$ on each j Bézier patch, we can find a solution at any point $x \equiv \{x_1, x_2, x_3\}$ of the domain based on the following integral identity [9]

$$u(x) = \sum_{j=1}^{n} \int_{v_{j-1}}^{v_j} \int_{w_{j-1}}^{w_j} \left\{ \hat{\overline{U}}_j^*(x,v,w) p_j(v,w) - \hat{\overline{P}}_j^*(x,v,w) u_j(v,w) \right\} J_j(v,w)\, \mathrm{d}v\, \mathrm{d}w, \tag{16}$$

together with the kernels

$$\hat{\overline{U}}_j^*(x,v,w) = \begin{bmatrix} \mathrm{Re}\{\hat{U}_j^*\} & -\mathrm{Im}\{\hat{U}_j^*\} \\ \mathrm{Im}\{\hat{U}_j^*\} & \mathrm{Re}\{\hat{U}_j^*\} \end{bmatrix}, \tag{17}$$

where

$$\hat{U}_j^* = \frac{1}{4\pi r} e^{ikr} = \frac{1}{4\pi r} \left\{ \cos kr + i \sin kr \right\},$$

and

$$\hat{\overline{P}}_j^*(x,v,w) = \begin{bmatrix} \mathrm{Re}\{\hat{P}_j^*\} & -\mathrm{Im}\{\hat{P}_j^*\} \\ \mathrm{Im}\{\hat{P}_j^*\} & \mathrm{Re}\{\hat{P}_j^*\} \end{bmatrix}, \tag{18}$$

where

$$\hat{P}_j^* = \frac{\partial \hat{U}_j^*}{\partial n} = \frac{1}{4\pi r^3} \left\{ (\cos kr + kr \sin kr) + i\,(\sin kr - kr \cos kr) \right\} \left\{ \overleftrightarrow{r}_1 n_1 + \overleftrightarrow{r}_2 n_2 + \overleftrightarrow{r}_3 n_3 \right\}.$$

The above formulas, just like (7)–(9) are similar to previously described in [9], where we dealt with the boundary modeled with the help of Coons patches. The difference lies in the fact that in

$$\begin{aligned} &\overleftrightarrow{r}_1 = x_1 - P_{j\{x_1\}}(v,w), \qquad \overleftrightarrow{r}_2 = x_2 - P_{j\{x_2\}}(v,w), \\ &\overleftrightarrow{r}_3 = x_3 - P_{j\{x_3\}}(v,w), \qquad r = \left[\overleftrightarrow{r}_1^2 + \overleftrightarrow{r}_2^2 + \overleftrightarrow{r}_3^2 \right]^{0.5}, \end{aligned} \tag{19}$$

we must substitute the formula (5) which represents the proposed triangular Bézier surfaces. Analogous adaptations must also be carried out for the Jacobian $J_j(v,w)$ and the normal derivatives $n_1 = n_1(v,w)$, $n_2 = n_2(v,w)$, $n_3 = n_3(v,w)$ currently given by (11)–(13).

5. Numerical examples

The practical aspects and the effectiveness of the proposed approach was tested on presented numerical examples. Figure 2 shows a closed spherical shell considered by the PIES as the boundary geometry in the two examples below.

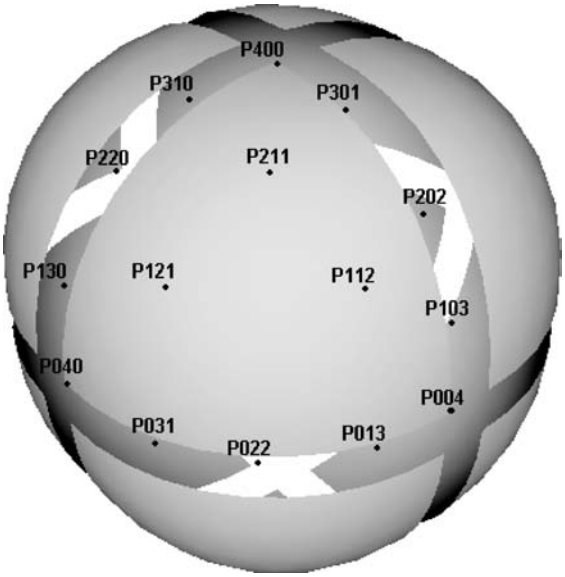

Fig. 2. A sphere approximated with 8 symmetrical triangular Bézier patches.

The sphere is approximated by eight symmetrical Bézier patches of 4th degree. However, this does not limit the shapes available in the algorithm. Every triangular patch used to approximate exactly 1/8 of the sphere is defined by 15 control points. The coordinates of control points $P_{ijk}\{x_1, x_2, x_3\}$ for Bézier patch placed in the first quadrant of the Cartesian coordinate system are shown below [11]

$$\begin{aligned}
&P_{004}\{0,1,0\} \quad P_{013}\{\alpha,1,0\} \quad P_{022}\{\beta,\beta,0\} \quad P_{031}\{1,\alpha,0\} \quad P_{040}\{1,0,0\}\\
&P_{103}\{0,1,\alpha\} \quad P_{112}\{\gamma,1,\gamma\} \quad P_{121}\{1,\gamma,\gamma\} \quad P_{130}\{1,0,\alpha\}\\
&P_{202}\{0,\beta,\beta\} \quad P_{211}\{\gamma,\gamma,1\} \quad P_{220}\{\beta,0,\beta\}\\
&P_{301}\{0,\alpha,1\} \quad P_{310}\{\alpha,0,1\}\\
&P_{400}\{0,0,1\}
\end{aligned} \tag{20}$$

where

$$\alpha = \frac{\left(\sqrt{3}-1\right)}{\sqrt{3}}, \qquad \beta = \frac{\left(\sqrt{3}+1\right)}{2\sqrt{3}},$$
$$\gamma = 1 - \frac{\left(5-\sqrt{2}\right)\left(7-\sqrt{3}\right)}{46}.$$

The outer edges of formed patches are joined together to form a closed sphere with satisfied the geometric continuity of the zeroth derivative along joining lines and with continuous curvature across the patches. As the result only 56 control points have been introduced to define the sphere.

5.1. Example 1

The first example focuses on the problem of propagation of sound waves in external infinite domain to a unit sphere with center at the origin. Dirichlet boundary conditions on a spherical surface are posed, given as a function from the following true solution [4]

$$u_1(r) = \frac{e^{ikr}}{r}, \quad \text{where} \quad r = \sqrt{x_1^2 + x_2^2 + x_3^2}. \tag{21}$$

We assume that the acoustic medium is the air with a temperature of 20°C and the speed of sound is roughly 344 m/s. For these parameters and the frequency of 100 Hz, parameter k takes the value 1.8265 [4].

Table 1 presents the percentage error of the PIES results to exact values (21) obtained at selected points in the external domain.

Table 1. Comparison of the exact (21) and numerical solutions in the PIES obtained at selected points of exterior domain.

Point	Exact solution (21)		Relative error [%] of the PIES solutions	
	Re	Im	Re	Im
1	2	3	4	5
(0,0,2)	−0.4360	−0.2447	0.0329	0.1046
(0,0,4)	0.1302	0.2133	0.0771	0.0845
(0,0,8)	−0.0572	0.1112	0.1742	0.0246
(0,0,−2)	−0.4360	0.2447	0.0329	0.1046

As has already been noticed, the PIES results are in excellent agreement with theoretically known values in both the near $(0, 0, 2)$ and further away $(0, 0, 8)$ from the boundary.

5.2. Example 2

The purpose of the second example is to examine the convergence of numerical solutions obtained in the algorithm. The tests were carried out by analysis of

external problem to a sphere of radius $r = 1$ with Dirichlet boundary conditions, obtained from more complicated comparing to the previous example two new functions [5]

$$u_2(x_1, x_2, x_3) = \frac{e^{ikr}}{r^2}\left(1 + \frac{i}{kr}\right) x_3, \tag{22}$$

$$u_3(x_1, x_2, x_3) = \frac{e^{ikr}}{r^3}\left(-1 + \frac{3}{k^2 r^2} - \frac{3i}{kr}\right) 0.5\left(3x_3^2 - r^2\right), \tag{23}$$

where $r = \sqrt{x_1^2 + x_2^2 + x_3^2}$.

Due to the fact that the PIES solutions on the boundary are approximated on each Bézier surface by series (14) and (15), the accuracy of the calculations significantly depends on the degree of Chebyshev polynomials [9] (and hence on the number $\overline{n} = N \times M$ of terms in the expressions (14), (15)). The number of terms $\overline{n} = N \times M$ may be varied on each Bézier patches, that form the boundary geometry. As we see in Tables 2, 3 the number of used Chebyshev polynomials has direct impact on the accuracy of solutions in the domain.

Table 2. Convergence of the PIES solutions in selected points in exterior domain for function u_2, $k = 2$.

Point	Exact solution (22)		Relative error [%] of the PIES solutions			
			288 equations		480 equations	
	Re	Im	Re	Im	Re	Im
1	2	3	4	5	6	7
(10,11,12)	0.0282	0.0168	0.1423	0.1381	0.0275	0.0306
(5,6,7)	−0.0361	0.0523	0.0986	0.1659	0.0270	0.0280
(1,2,3)	0.0506	0.2098	0.5805	0.1016	0.1282	0.0011

Table 3. Convergence of the PIES solutions in selected points in exterior domain for function u_3, $k = 2$.

Point	Exact solution (23)		Relative error [%] of the PIES solutions			
			288 equations		480 equations	
	Re	Im	Re	Im	Re	Im
1	2	3	4	5	6	7
(10,11,12)	−0.0039	−0.0026	0.7242	3.7394	0.2596	0.3904
(5,6,7)	0.0103	−0.0123	1.6450	0.4877	0.1210	0.2499
(1,2,3)	0.0038	−0.1274	9.4040	0.2181	2.7842	0.1195

Columns 4, 5 in both these tables contain the solutions obtained for $\overline{n} = 9$ terms in each of the 8 triangular Bézier patches. In this case, a total set of 288 algebraic equations must be solved. The obtained results are in good agreement with

the theoretical values for both functions u_2, u_3 at selected measurement points (columns 2, 3). To examine the convergence of solutions, the same problem was solved again by introducing more terms of approximation series for $\overline{n} = 15$, with total number of 480 algebraic equations to be solved. The obtained solutions can be found 6, 7 in both tables with a much smaller error lever. Improving the accuracy of the solutions by increasing the number of approximate series is very effective, because it is carried out without any modification of represented by 8 Bézier patches boundary geometry.

6. Conclusions

Presented algorithm for numerical solving 3D Helmholtz equation by the PIES not only simplifies the way of modelling the boundary geometry but also allows to obtain solutions with high accuracy and provides an effective mechanizm to study the convergence of solutions. Triangular Bézier patches can not be identified with boundary element, known from the BEM. Firstly, the patches are directly linked in mathematical formalism of the PIES. Moreover, it is required to use a much smaller number of such patches, compared with boundary elements. Despite the fact that the boundary elements have parametric representation, the direct BEM solution is obtained at nodal points only, associated with declared boundary elements. Therefore, in order to obtain solutions to a greater number of points, we must divide the boundary under consideration for a larger number of boundary elements. The number of such nodes is also much higher in comparison with the declared in the case of 56 control points of 8 Bézier patches. The numerical examples show that the presented approach is characterized by high accuracy of solutions.

References

[1] Ciskowski R.D., Brebbia C.A., *Boundary Element Methods in Acoustics*, Elsevier Applied Science, New York 1991.

[2] Farin G., *Computer Aided Geometric Design (CAGD)*, Academic Press, New York 1996.

[3] Kiciak P., *Podstawy modelowania krzywych i powierzchni*, WNT, Warszawa 2000.

[4] Kirkup S., *The Boundary Element Method in Acoustics*, Integrated Sound Software 1998.

[5] Lin T.C, Warnapala–Yehiya Y., *The numerical solution of the exterior dirichlet problem for Helmholtz's equation via modified green's functions approach*, Computers & Mathematics with Applications, **44**, 8–9, 1229–1248 (2002).

[6] Zieniuk E., *Modelling and effective modification of smooth boundary geometry in boundary problems using B-spline curves*, Engineering with Computers, **23**, 39–48 (2007).

[7] Zieniuk E., Bołtuć A., *An algorithm for numerical solving of the two-dimensional Helmholtz equation using a parametric integral equations systems (PIES)*, Structures Waves Human Health, **13**, 1, 157–164 (2004).

[8] Zieniuk E., Bołtuć A., *Non-element method of solving 2D boundary problems defined on polygonal domains modeled by Navier equation*, International Journal of Solids and Structures, **43**, 7939–7958 (2006).

[9] Zieniuk E., Szerszeń K., *A solution of 3D Helmholtz equation for boundary geometry modeled by Coons patches using the Parametric Integral Equation System*, Institute of Fundamental Technological Research PAN, Archives of Acoustics, **31**, 99–111 (2006).

[10] Zienkiewicz O., *The Finite Element Methods*, McGraw-Hill, London 1977.

[11] Youg-Qing L., Ying-Lin K., Wei-Shi L., *Termination criterion for subdivision of triangular Bézier patch*, Computer and Graphics, **26**, 67–74 (2002).